RSC Advances

PAPER

View Article Online
View Journal | View Issue

Cite this: *RSC Adv.*, 2024, **14**, 6135

Shrimp oil nanoemulsions prepared by microfluidization and ultrasonication: characteristics and stability

Bharathipriya Rajasekaran,[a] Avtar Singh,[a] Krisana Nilsuwan,[a] Lukai Ma,[b] Rasool Abdul Nazeer*[c] and Soottawat Benjakul *[ad]

Shrimp oil (SO) nanoemulsions stabilized by fish myofibrillar protein, considered as functional foods, were prepared *via* microfluidization and ultrasonication. The study explored varying microfluidization (pressure and cycles) and ultrasonication (amplitude and sonication time) conditions that influenced emulsion properties and stability. Ultrasonicated emulsions exhibited superior emulsifying properties, adsorbed protein content, thermal stability, and centrifugal stability than microfluidized emulsions ($p < 0.05$). Microfluidization at 6.89 and 13.79 MPa with 2 or 4 cycles yielded larger droplets (536 to 638 nm) ($p < 0.05$), while ultrasonication at 40% and 50% amplitude for 5, 10 and 15 min produced smaller droplets (426 to 494 nm) ($p < 0.05$). Optimal conditions were obtained for microfluidization (13.79 MPa, 2 cycles) and ultrasonication (50% amplitude, 10 min). Ultrasonicated emulsions had generally smaller d_{32} and d_{43}, lower polydispersity and higher ζ-potential than their microfluidized counterparts. Microstructural analysis and CLSM images confirmed their superior stability during storage. SO nanoemulsions could be applied as functional food.

Received 28th October 2023
Accepted 2nd February 2024

DOI: 10.1039/d3ra07342d

rsc.li/rsc-advances

1. Introduction

In recent years, individuals have been increasingly focused on health and disease prevention, leading to rising demand for food products enriched with functional ingredients.[1] Furthermore, waste from shrimp processing industries has received considerable interest due to the presence of notable bioactive substances such as polyunsaturated fatty acids (PUFA), astaxanthin and chitin derivatives.[2] The oil extracted from shrimp hepatopancreas is particularly abundant in n-3 fatty acids, astaxanthin, fat-soluble vitamins and phospholipids.[3] Several studies have extensively demonstrated the health benefits associated with shrimp oil (SO) consumption. However, the incorporation of lipophilic ingredients directly into food products is challenging due to their poor solubility and vulnerability to lipid oxidation.[4] Thus, extensive efforts have been made to overcome these challenges to fulfill the growing demand for functional foods. Previous reports have shown that delivery systems such as emulsion, oleo gel, microcapsule and nanoliposome can protect bioactive compounds from adverse environments and enhance their bioavailability during digestion.[5] Several natural and processed food products such as milk, butter, soups, sausage, sauces, ice cream, salad dressing, mayonnaise, *etc.* have been known as food emulsions.[6] Emulsions are thermodynamically unstable. Therefore, active emulsifiers are employed to stabilize the emulsion. Proteins are amphiphilic molecules with surface-active properties that preferably adsorb at the interface and prevent droplet coalescence, stabilizing the emulsion.[7]

Fish meat is rich in protein and often used for consumption or processing into several products. Fish myofibrillar protein (FMP) is a major constituent of fish meat and exhibits excellent functional properties. FMP has the potential to be used as an emulsifier in the production of SO-in-water emulsions.[8] FMP possesses two globular heads and a rod like α-helical tail. The myosin in FMP forms interfacial film by partially unfolding its head domain and α-helical tail, exposing active sites such as hydrophobic and sulfhydryl groups. The unique structure of FMP allows it to act as an emulsifier by adsorbing onto oil droplets. Simultaneously, the tail portion of myosin contributes to forming a network structure in the aqueous phase, thus aiding in stabilization.[7] This could be advantageous for the food industry as it allows for the production of functional food emulsions with high nutritional value and nutraceutical properties. Nanoemulsions are another type of emulsion having

[a]*International Center of Excellence in Seafood Science and Innovation, Faculty of Agro-Industry, Prince of Songkla University, Hat Yai, 90110, Songkhla, Thailand. E-mail: soottawat.b@psu.ac.th*

[b]*Key Laboratory of Green Processing and Intelligent Manufacturing of Lingnan Specialty Food of Ministry and Rural Affairs, College of Light Industry and Food, Zhongkai University of Agriculture and Engineering, Guangzhou 510225, China*

[c]*Biopharmaceuticals Lab, Department of Biotechnology, School of Bioengineering, SRM Institute of Science and Technology, Kattankulathur, Chennai 603203, Tamil Nadu, India. E-mail: nazeerr@srmist.edu.in*

[d]*Department of Food and Nutrition, Kyung Hee University, Seoul 02447, Republic of Korea*

small droplet sizes ranging from 100 to 1000 nm.[9] They offer various benefits over conventional emulsions such as great stability, visual clarity and increased bioavailability of encapsulated compounds, making them appropriate for the food, beverage, and pharmaceutical sectors.[10] Moreover, the high physical stability of the nanoemulsion is largely determined by the small and homogenous distribution of oil droplets during emulsification.[11] Therefore, an effective emulsification technique is necessary to produce nanoemulsions that retain their quality for an extended period. Among various emulsification techniques, microfluidization and ultrasonication have been recognized as efficient methods due to their ability to produce fine emulsions with desired functional properties.[12]

Microfluidization is a high-pressure homogenization technology capable of producing homogeneous particles with reduced size. As a fluid passes through an interaction chamber, the microfluidizer generates strong shear and impact forces that induce the creation of tiny droplet emulsion.[13] On the other hand, ultrasonication creates sound waves that dissipate through liquid media, resulting in cavitation effect and its efficacy depends on the frequency used. The pressure cycle causes small voids in the liquid which eventually collapse during the high-pressure cycle, resulting in high localized turbulence, shear forces, pressures, and temperatures.[14] Microfluidization combines the intense shear rate, high-frequency vibration, and hydrodynamic cavitation, while ultrasonication utilizes ultrasonic waves to create acoustic cavitation.[11] Since SO is rich in n-3 fatty acids and astaxanthin, it can be used as a functional emulsion for food uses. SO emulsion with FMP aims to mimic the composition of real food models *e.g.* mayonnaise. Astaxanthin is a pigment in SO resembling the color of egg yolk and the myofibrillar protein (FMP) acts as an emulsifier which is known for its salt solubility and amphiphilic nature. Given the health risks associated with excessive salt intake, acetic acid solution was used to solubilize FMP *via* protonation. The selection of low pH mimics food emulsion, where vinegar is a key ingredient. Despite the familiarity of microfluidization and ultrasonication in emulsion preparation, their comparison and information regarding the effect of homogenization techniques on the production of nanoemulsion remains scarce. Therefore, the objective of this study was to produce and evaluate the effect of different homogenization techniques (microfluidizer and ultrasound) under varying operating conditions on the emulsifying, physical properties, and stability of SO nanoemulsions. This study addresses this gap by systematically evaluating the effectiveness of homogenization techniques, particularly in the context of SO nanoemulsions stabilized by FMP, a novel combination with significant implications for functional food development.

2. Materials and methods

2.1. Chemicals

Analytical grade chemicals were obtained from Sigma (St. Louis. MO, USA). Solvents were procured from ACI Lab-scan (Bangkok, Thailand). Soybean oil (SBO) was acquired from a local supermarket situated in Hat Yai, Songkhla, Thailand.

2.2. Extraction of oil from the hepatopancreas of shrimp

The frozen hepatopancreas sourced from freshly caught Pacific white shrimp (*Litopenaeus vannamei*) and preserved at −20 °C was generously provided by Seafresh Industry Public CO., Ltd (Chumphon, Thailand). SO was extracted from the hepatopancreas paste following the protocol outlined by Gulzar and Benjakul.[12]

2.3. Preparation of fish myofibrillar protein and its solution

Fresh Asian seabass was obtained from a local market in Hat Yai (3–4 h after capture). When the fish arrived, they were cleaned, filleted, and minced with a blender. Mince was prepared, thoroughly rinsed with cold distilled water (4 °C) and filtered using a cheesecloth. The washing process was repeated three times and centrifuged (3000 × *g*, 15 min, 4 °C) to obtain the concentrated myofibrillar protein.[15]

To prepare the FMP solution, the pellets were homogenized (13 000 rpm, 1 min) in distilled water. The 50% acetic acid was gradually added to the homogenate while stirring for 10 min to obtain a pH of 3.0. The homogenate was then refrigerated at 4 °C overnight with continuous stirring to ensure complete solubilization. To eliminate any remaining undissolved substances, the centrifugation (10 000 × *g*, 20 min, 4 °C) of solution was done. The resulting supernatant was designated as fish myofibrillar protein (FMP). According to our previous research, a FMP concentration of 15 mg mL^{-1} was the optimal level to produce a stable SO-in-water emulsion.[8] Biuret method was used to determine the protein content of the FMP, in which BSA was used as the standard.[16]

2.4. Preparation of shrimp oil-in-water emulsion

2.4.1. Coarse emulsion preparation. SO-in-water emulsions were prepared. FMP solution (15 mg mL^{-1}) containing 0.02% sodium azide was served as the aqueous phase. The oil phase was composed of a mixture of SO and SBO (30 : 70, v/v), specifically chosen to mitigate the fishy odor associated with SO.[8] Emulsion preparation involved a two-stage process. In the initial stage, coarse emulsions were prepared, in which 10 mL of the SO/SBO mixture was homogenized with 30 mL of FMP at 11 000 rpm for 2 min at 4 °C.[17] Subsequently, the coarse emulsion was homogenized by either a microfluidizer or an ultrasound probe.

2.4.2. Microfluidization. The freshly prepared coarse emulsion was further subjected to high-pressure microfluidizer (Microfluidics, Model HC-5000, Stanwood, WA, USA) at pressures of 6.89 and 13.79 MPa for 2 and 4 passes. For each treatment, 200 mL of coarse emulsion was processed through the microfluidizer for two passes. After this initial processing, one-third of the micro-fluidized sample was collected for analysis. The remaining volume of the sample was subsequently microfluidized for an additional two passes using the microfluidizer.[18]

2.4.3. Ultrasonication. The coarse emulsion underwent an ultrasonication process using an ultrasonic processor (Sonics, Model VC 750, Sonic and Materials, Inc., Newtown, CT, USA) at a frequency of 20 kHz ± 50 Hz and high-intensity power of

750 W. During ultrasonication, the emulsion was exposed to different amplitudes, including 40% and 50%, for varying durations (5, 10 and 15 min). Temperature was maintained below 10 °C, by placing the sample in the iced bath. The ultrasonication was performed in a pulse mode (2s-on and 4s-off).[19] All the emulsions were immediately used for further analyses.

2.5. Characterization of SO-in-water emulsions

2.5.1. Emulsifying properties. Emulsion activity index (EAI) and emulsion stability index (ESI) were determined immediately after the emulsion was prepared. To assess these indices, samples were taken from the bottom of the tubes at 0 and 30 min.[20] Subsequently, these samples were 2000-fold diluted using a solution consisting of 1% (v/v) acetic acid and 0.1% (w/v) SDS (AA-SDS). To prevent flocculation, the mixture was vigorously vortexed for 5 s. The absorbance at 500 nm was then read using a spectrophotometer (UV-160, Shimadzu, Kyoto, Japan).

$$\mathrm{EAI}\left(\mathrm{m^2\ g^{-1}}\right) = \frac{2 \times 2.303 \times A_0 \times \mathrm{DF}}{C \times L \times (1 - \varnothing) \times 10\,000}$$

$$\mathrm{ESI(min)} = \frac{A_0 \times \Delta t}{A_0 - A_{30}}$$

where A_0 and A_{30} represent the absorbance measured at 0 and 30 min, respectively. DF stands for the dilution factor, while L represents the path length of the cuvette in meters. C denotes the initial protein concentration (g $\mathrm{mL^{-1}}$). $\varnothing$ signifies the oil volume fraction (0.25). Lastly, Δt represents the time interval (30 min).

2.5.2. Adsorbed protein content (APC). The method of Silva *et al.*[21] was adopted for assessment of APC of the freshly prepared SO-in-water emulsions. Five mL of the emulsion were subjected to centrifugation (10 000 × g for 1 h, 25 °C). After centrifugation, the oil droplets in the top phase were carefully removed, leaving the unabsorbed protein in the bottom phase, in which protein content (C_S) was determined using the Biuret method. In a similar manner, aqueous FMP was centrifuged under identical conditions and the protein content in the resulting supernatant (C_A) was also examined. The initial protein concentration of FMP before centrifugation was denoted as CI. APC was computed as follows:

$$\mathrm{APC}\ (\%) = [(C_A - C_S)/C_I] \times 100$$

2.5.3. Thermal and centrifugal stability. To assess thermal stability, emulsions were heated in a water bath at 100 °C for 20 min and then cooled to room temperature (25 °C) within 30 min.[22] ESI was then evaluated. For centrifugal stability, 5 mL of emulsion was subjected to centrifugation (3500 × g, 15 min). Centrifugal stability was calculated and expressed in percentages as guided by Gulzar and Benjakul.[12]

$$\text{Centrifugal stability} = \frac{A - B}{A} \times 100$$

where A is initial volume of emulsion before centrifugation and B is volume of bottom phase after centrifugation.

2.5.4. Droplet size, polydispersity index (PDI), zeta (ζ) potential and flocculation index (F_i). Droplet size, PDI, F_i and ζ-potential were determined using a Zeta potential analyzer (ZetaPlus, Brookhaven Instruments Corporation, Holtsville, NY, USA). Before droplet size analysis, the emulsion was diluted 100-fold with a solution containing 1% (v/v) AA-SDS to disperse any flocculated droplets.[23] To ensure the accurate measurements, the manufacturer's recommendations were followed, including setting the refractive index at 1.330 and the absorption at 0.001. The calculation of F_i was based on the d_{43} as described by Benjakul *et al.*[24]

$$F_i = \frac{d_{43} - \mathrm{SDS}}{d_{43} + \mathrm{SDS}}$$

where d_{43} − SDS and d_{43} + SDS represent droplet diameter (d_{43}) without and with the addition of 1% (w/v) SDS, respectively.

2.5.5. Microstructure. An optical microscope (Olympus IX70 with DP50, Shinjuku, Tokyo, Japan) was used to analyze the microstructure of the emulsion.[11] All observations were made at a magnification of 40×.

2.5.6. Confocal laser scanning microscopic image (CLSM). CLSM was conducted using an Olympus confocal microscope (Model FV300, Tokyo, Japan).[25] Before performing the analyses, the emulsion was combined with Nile blue A at a 1 : 5 ratio and manually stirred until uniformity was achieved. A 50 μL mixture was placed on a slide and covered with a cover slip. To analyze lipids, a fluorescence mode was utilized, employing an excitation wavelength of 533 nm and an emission wavelength of 630 nm. A Helium–Neon Red laser (HeNe-R) was used and observations were made at a magnification of 400×.

2.6. Statistical analysis

All experiments and analyses were conducted in triplicate. A completely randomized design (CRD) approach was implemented. The data were subjected to analysis of variance (ANOVA). Subsequently, Duncan's multiple range test was employed to compare means. Statistical analysis was performed using SPSS-23 software (SPSS Inc., Chicago, IL, USA).

3. Results and discussion

3.1. Emulsifying properties

EAI and ESI of the SO nanoemulsion prepared using different emulsification techniques with varying operating conditions are given in Fig. 1A and B, respectively. When comparing two emulsification techniques, ultrasonicated emulsion generally exhibited superior emulsifying properties than microfluidized emulsion under the conditions used in the present study ($p < 0.05$). Overall, emulsion ultrasonicated at 50% amplitude for 10 min had the highest EAI and ESI ($p < 0.05$), whereas microfluidized emulsion at 13.69 MPa for 2 passes showed greater emulsifying properties than the rest of microfluidized emulsion samples ($p < 0.05$). EAI evaluates the protein's capacity to quickly adsorb on the surface of oil droplets to create and

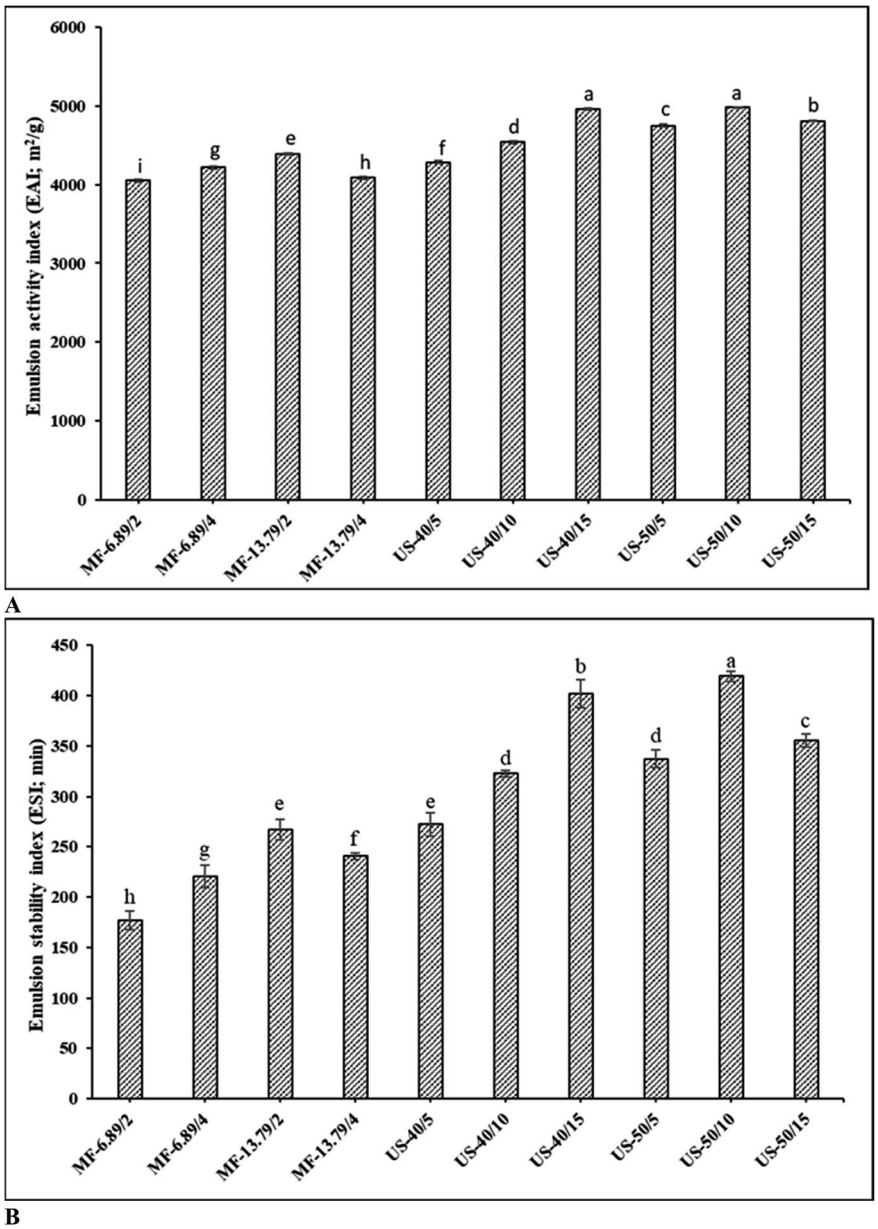

Fig. 1 Emulsion activity index, EAI (A) and emulsion stability index, ESI (B) of SO nanoemulsions stabilized by fish myofibrillar protein (FMP) prepared using microfluidization and ultrasonication under varying operating conditions. MF-6.89/2, MF-6.89/4, MF-13.79/2, MP-13.79/4: SO nanoemulsions microfluidized at 6.89 MPa and 13.79 MPa for 2 and 4 cycles, respectively. US-40/5, US-40/10, and US-40/15, US-50/5, US-50/10, US-50/15: SO nanoemulsions ultrasonicated at 40% and 50% amplitude for 5, 10 and 15 min, respectively. Different lowercase letters on the bar denote significant differences ($p < 0.05$). Bars represent the standard deviations ($n = 3$).

stabilize the oil–water interface during homogenization.[26] The ability of emulsion to resist phase separation and sustain smaller and uniform droplet dispersion is referred to as ESI.[27]

For microfluidization, the increases in number of passes from 2 to 4 at 6.89 MPa, EAI and ESI upsurged ($p < 0.05$). When 2 passes were used, EAI and ESI increased as the pressure augmented from 6.89 to 13.79 MPa ($p < 0.05$) (Fig. 1). This increase was plausibly due to the disruption effect of droplets caused by turbulent flow and cavitation.[28] Higher disruption of droplets was related to more stable emulsion. During microfluidization, the coarse emulsion is pumped at high pressure into an interaction chamber, where it is divided into two or more microstreams and collides with each other, resulting in a fine emulsion with small droplets.[11] With the increasing pressure and number of passes, the microstream collides at high velocity due to an increase in energy input, thus leading to an enhanced disruption effect in the microfluidized emulsion.[7] However, a slight reduction in both EAI and ESI was observed when 4 passes were applied than 2 passes at the pressure of 13.79 MPa ($p < 0.05$). This phenomenon might be related to the over-processing effect. When emulsion is microfluidized with a high energy input beyond a critical point, Brownian motion

increases, thereby increasing the possibility of droplet collision and re-coalescence.[11] In addition, the droplet breakdown rate exceeds the protein adsorption rate at the interface. Consequently, the emulsifier cannot sufficiently cover the oil droplet surface, leading to re-coalescence as witnessed by lowered emulsifying properties.[29]

Among ultrasonicated samples, emulsion formed at 50% amplitude for 10 min had the highest EAI and ESI ($p < 0.05$), while 40% amplitude for 5 min resulted in the lowest EAI and ESI ($p < 0.05$). The latter was attributed to the insufficient quantum of energy to disperse the oil phase into the aqueous phase.[30] At 40% amplitude, EAI and ESI increased with augmenting sonication time from 5 to 15 min ($p < 0.05$). Furthermore, increasing the ultrasound amplitude from 40% to 50% improved both EAI and ESI, regardless of sonication time ($p < 0.05$). This was because of the difference in droplet breakage during ultrasonication. Increased energy input might create a greater amplitude of ultrasonic waves to pass through the emulsion, resulting in a more violent bubble collapse.[19] This produced emulsion with small and uniformly dispersed droplets with high emulsion stability. Energy dissipated during ultrasonication primarily depends on ultrasound amplitude and sonication time.[31] During ultrasonication, bubbles collapse, thus releasing a burst of energy, which leads to increased pressure and temperature in the local spot. Local temperature represents only specific spot, where the bubble is burst and does not reflect the overall temperature of the medium.[29] To counteract the temperature rise during cavitation, ultrasound treatment was done under controlled temperature in iced bath. Temperature was maintained below 10 °C during ultrasonication. Moreover, pulsing mode (2s-on and 4s-off) was applied to control the rise in temperature.[8] Nevertheless, emulsifying properties decreased, when coarse emulsion was subjected to ultrasound at 50% amplitude longer than 10 min ($p < 0.05$). The result suggested that 50% amplitude for 10 min was an optimal operating condition for ultrasonication of SO nanoemulsion. Harsh conditions (50% amplitude, 15 min) contributed to the accelerated coalescence. This coalescence occurred due to high treatment power, which might increase the local temperature of the sample. Furthermore, the rapid temperature upsurge adversely affected the emulsion system, leading to collisions, aggregation, and fusion of some oil droplets.[11] In addition, high energy input beyond the optimum conditions could lead to excessive protein unfolding or denaturation. Subsequently, protein–protein interaction between exposed hydrophobic domains could occur *via* hydrophobic interactions.[14] Moreover, droplet disruption was superimposed by droplet re-coalescence at high energy input, resulting in the increased droplet size.[11]

3.2. Adsorbed protein content (APC)

APC of SO nanoemulsion prepared using different homogenization techniques is given in Fig. 2. Among all tested samples, ultrasonicated emulsion had higher APC when 50% amplitude was applied for 10 min ($p < 0.05$). Generally, a higher amount of adsorbed protein improves emulsion stability.[28] For microfluidization, APC increased with augmenting number of microfluidization passes from 2 to 4 when the pressure of 6.89 MPa was used ($p < 0.05$). This was attributed to the breakdown of droplets into smaller sizes after repeated microfluidization passes in the interaction chamber. Thus, proteins could migrate to oil droplets and adsorb to a higher extent. Additionally, pressure unfolds and alters the tertiary and quaternary structure of protein during microfluidization which facilitates its adsorption over oil droplets.[13] The partial unfolding and conformational changes of protein caused by microfluidization facilitated the exposure of hydrophobic residues. This could favor the binding ability of protein to the surface of oil droplets.[28] However, as the pressure of 13.79 MPa was used, APC decreased as the number of microfluidization passes increased from 2 to 4 cycles ($p < 0.05$). This might be owing to an extensive denaturation of FMP under high hydrostatic pressure. FMP consists of globular head and the rod-like alpha helical tail. The excessive unfolding of head domain caused by high pressure could lead to the protein aggregation *via* hydrophobic interactions.[32] As a consequence, large aggregate could not migrate to the interface effectively. Generally, protein adsorption at the interface is influenced by size, surface hydrophobicity, and flexibility of protein molecules. Protein aggregation lowers its flexibility, thus hindering the diffusion from the aqueous phase to the interface as well as rearrangement over the oil droplets at the interface.[26]

When ultrasonication at 40% amplitude was employed, APC increased noticeably as the ultrasonication time augmented from 5 to 15 min ($p < 0.05$). Cavitation reduced the size of oil droplets and enhanced their surface area. Additionally, longer sonication time might improve the solubility of proteins, thereby increasing their adsorption rate at the oil–water interface.[22] Solubility gradually increased with the augmenting ultrasonication time due to reduction in the size of protein. Smaller size of the protein has enhanced diffusion from the aqueous phase and can adsorb at the interface during emulsification. This resulted in more adsorbed protein per unit interfacial area of the emulsion. Therefore, high adsorbed protein led to more stable emulsion.[8] Moreover, increased protein adsorption resulted in the production of multilayered, densely packed and thick interfacial film, which enhanced emulsion stability.[33] This result was in accordance with the ESI (Fig. 1B). High APC indicated that more proteins were adsorbed per unit interfacial area.[20] However, there was a slight decrease in APC when ultrasonication time upsurged from 10 to 15 min at 50% amplitude. Prolonged treatment at a high-power level might intensify the sonochemical effects and disrupt the secondary structure of protein, resulting in the formation of insoluble protein aggregates.[34] Hence, processing parameters applied during homogenization had a profound influence on APC of SO nanoemulsion.

3.3. Thermal and centrifugal stabilities

Thermal and centrifugal stabilities of SO nanoemulsions prepared by different homogenization techniques are given in

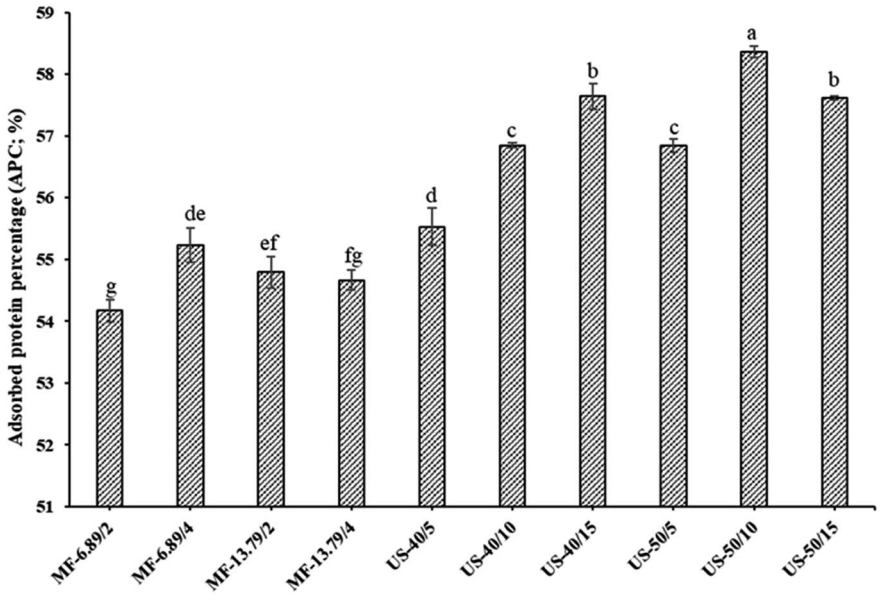

Fig. 2 Adsorbed protein content of SO nanoemulsions stabilized by fish myofibrillar protein (FMP) prepared using microfluidization and ultrasonication under varying operating conditions. MF-6.89/2, MF-6.89/4, MF-13.79/2, MP-13.79/4: SO nanoemulsions microfluidized at 6.89 MPa and 13.79 MPa for 2 and 4 cycles, respectively. US-40/5, US-40/10, and US-40/15, US-50/5, US-50/10, US-50/15: SO nanoemulsions ultrasonicated at 40% and 50% amplitude for 5, 10 and 15 min, respectively. Different lowercase letters on the bar denote significant differences ($p < 0.05$). Bars represent the standard deviations ($n = 3$).

Fig. 3A and B, respectively. Heat applied during production and processing can alter the protein's interfacial behavior and aggregation. Thermal stability is therefore crucial to produce heat stable emulsion.[22] After heating, all emulsions were relatively stable without visible creaming or phase separation. This revealed that emulsions were resistant to heat processing, which might be due to the fact that temperature had no effect on steric or electrostatic repulsion between droplets.[35] Among all tested samples, emulsion ultrasonicated at 50% amplitude for 10 min had the highest thermal stability ($p < 0.05$). This was related to the greater adsorption of protein at the interface associated with electrostatic and steric repulsions.[36] Electrostatic repulsion arises from the electric charges on the protein covering the oil droplets, pushing them apart and preventing droplets from merging. Meanwhile, steric repulsion (loop configuration) arises from physical barriers or structure on the droplets surface, inhibiting proteins from getting too close and impeding coalescence.[18] These forces are essential in keeping droplets apart in the emulsion system, which is crucial to maintain the stability. The greater adsorption of proteins at the interface is associated with augmented electrostatic and steric repulsion.[8] The result was in line with the higher APC on oil droplets (Fig. 2). During heating, FMP macromolecules cross-link and aggregate on the surface of the oil droplets could form strong and dense interfacial film.[8] Typically, thermal stability is related to the hydrodynamic diameter of droplets and the interfacial loading of protein. Furthermore, lower hydrodynamic diameter primarily contributed to stronger interfacial loading, resulting in an effective stabilization of emulsion with less coarsening under high temperatures.[21] On the other hand, the thermal stability was lower in the emulsion microfluidized at 6.89 MPa for 2 passes and ultrasonicated at 40% for 5 min ($P < 0.05$). This could be due to the weaker electrostatic repulsion between the oil droplets due to lower protein adsorption, especially when heat was applied.

Centrifugation is a practical method to evaluate the coalescence stability of the emulsion. When the emulsion is exposed to centrifugal force, it causes the droplets to collide with each other, and the ability of the emulsion to withstand the pressure can be measured.[12] In general, the emulsion showed reduced stability after centrifugation, indicating the occurrence of creaming. Ultrasonicated emulsion had higher centrifugal stability than microfluidized emulsion ($p < 0.05$). Ultrasonicated emulsion (50% amplitude, 10 min) had the highest centrifugal stability, indicating a thick interfacial layer with lower interfacial tension between the oil and water phase ($p < 0.05$). The centrifugal stability of ultrasonicated emulsion ranged from 79.6% to 95.6% ($p < 0.05$). On the other hand, microfluidized emulsion exhibited lower centrifugal stability (71.1–76.3%) ($p < 0.05$). Centrifugal stability increased with augmenting amplitude and duration for ultrasonication, except when extreme condition (50% amplitude, 15 min) was used, in which centrifugal stability became lower. Pressure and number of passes for microfluidization also had varying impacts on centrifugal stability, when the harsh condition (13.79 MPa, 4 passes) was adopted. The detrimental effect enhanced protein–protein interaction or aggregation, thus lowering ability to cover oil droplets. This was also attributed to reduced protein adsorption, larger oil droplets, and lower viscoelasticity interfacial film, which reduced mechanical strength. Random collisions during centrifugation and eventual merging of emulsifiers from two or more droplets induce emulsion instability.[1] Under optimal conditions, protein–lipid interactions could

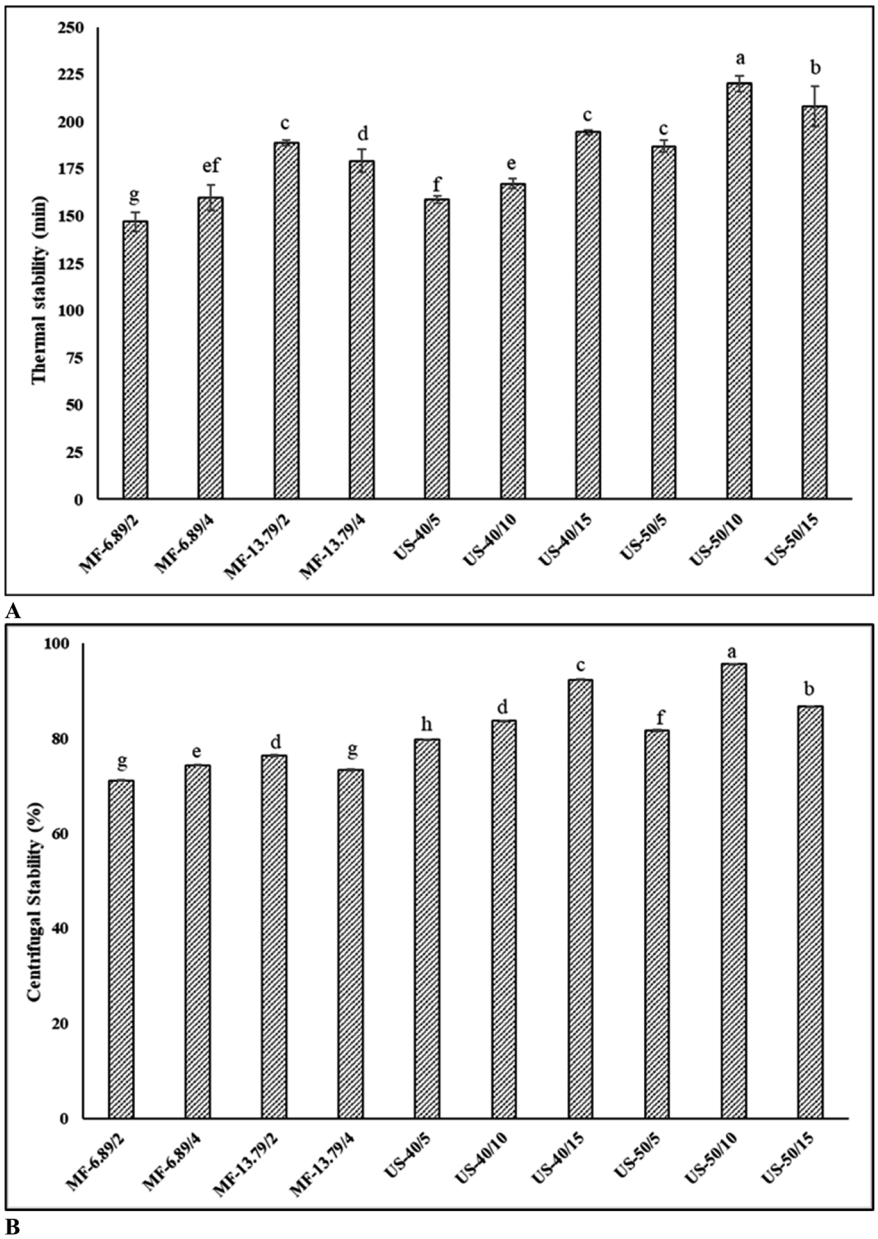

Fig. 3 Thermal stability (A) and centrifugal stability (B) of SO nanoemulsions stabilized by fish myofibrillar protein (FMP) prepared using microfluidization and ultrasonication under varying operating conditions. MF-6.89/2, MF-6.89/4, MF-13.79/2, MP-13.79/4: SO nanoemulsions microfluidized at 6.89 MPa and 13.79 MPa for 2 and 4 cycles, respectively. US-40/5, US-40/10, and US-40/15, US-50/5, US-50/10, US-50/15: SO nanoemulsions ultrasonicated at 40% and 50% amplitude for 5, 10 and 15 min, respectively. Different lowercase letters on the bar denote significant differences ($p < 0.05$). Bars represent the standard deviations ($n = 3$).

prevent the separation of oil phases from the aqueous phase containing protein during centrifugation. Moreover, FMP is self-assembled on the surface of the droplets and effectively prevents coalescence.[37] Therefore, processing parameters were crucial to obtain the desired stability of SO nanoemulsion.

3.4. Droplet size and PDI

Surface-weighted mean diameter (d_{32}), volume-weighted mean diameter (d_{43}) as well as PDI of the emulsions prepared with varying operating conditions are shown in Table 1. Droplet size is an important factor for evaluating the stability of the emulsion. PDI is related to the distribution homogeneity of oil droplet size. When the PDI value is close to zero, the droplet distribution is more uniform.[28] Under the selected condition, ultrasonicated emulsion (50% amplitude, 10 min) had smaller droplet size with lower PDI than its microfluidized counterpart (13.79 MPa, 2 passes) ($p < 0.05$). For microfluidization, droplet diameter is the function of microfluidizer pressure, emulsion composition and number of passes.[11] Increases in microfluidization pressure (6.89 to 13.79 MPa) and number of cycles (2 to 4) resulted in fine emulsion with narrow droplet distributions (497–637 nm) ($p < 0.05$). This could be due to the

Table 1 Droplet size, zeta (ζ) potential, polydispersity index (PDI) and flocculation index (F_i) of shrimp oil nanoemulsions stabilized by fish myofibrillar protein prepared using microfluidization and ultrasonication under varying operating conditions[a]

Homogenization	d_{32} (nm)	d_{43} (nm)	ζ-potential (mV)	PDI	F_i
MF-6.89/2	638.68 ± 0.27^{a}	647.87 ± 2.83^{a}	15.80 ± 0.15^{i}	0.265	2.11
MF-6.89/4	596.84 ± 1.84^{b}	600.65 ± 3.54^{b}	17.64 ± 0.23^{h}	0.255	2.15
MF-13.79/2	536.59 ± 1.00^{d}	540.30 ± 2.83^{d}	20.42 ± 0.21^{f}	0.226	2.01
MF-13.79/4	557.94 ± 1.28^{c}	562.85 ± 2.56^{c}	18.18 ± 0.14^{g}	0.239	2.07
US-40/5	494.49 ± 1.61^{e}	499.35 ± 1.41^{e}	22.74 ± 0.21^{e}	0.189	1.72
US-40/10	474.14 ± 3.28^{f}	480.32 ± 2.12^{f}	24.00 ± 0.35^{d}	0.155	1.54
US-40/15	438.70 ± 1.64^{i}	442.36 ± 3.54^{h}	26.24 ± 0.21^{b}	0.147	1.46
US-50/5	469.49 ± 1.56^{g}	473.67 ± 4.24^{f}	24.58 ± 0.14^{c}	0.165	1.37
US-50/10	426.89 ± 1.79^{j}	430.62 ± 2.83^{i}	28.94 ± 0.06^{a}	0.137	1.26
US-50/15	447.56 ± 2.25^{h}	452.15 ± 4.24^{g}	26.17 ± 0.32^{b}	0.146	1.33

[a] The values are presented as mean ± SD ($n = 3$). Different lowercase superscripts in the same column indicate significant differences ($p < 0.05$). MF-6.89/2, MF-6.89/4, MF-13.79/2, MP-13.79/4: SO nanoemulsions microfluidized at 6.89 MPa and 13.79 MPa for 2 and 4 cycles, respectively. US-40/5, US-40/10, and US-40/15, US-50/5, US-50/10, US-50/15: SO nanoemulsions ultrasonicated at 40% and 50% amplitude for 5, 10 and 15 min, respectively.

effective droplet disruption by microfluidizer. The result indicated that PDI decreased proportionally to energy input.[38] However, a slight increase in droplet size and PDI was observed in microfluidized emulsion at 13.79 MPa for 4 passes ($p < 0.05$). Higher PDI values might be associated with destabilization phenomena such as droplet flocculation. However, this occurrence was insufficient to cause creaming or phase separation. Typically, both droplet disruption and re-coalescence determine the final droplet size during microfluidization.[12] Because of the high energy input (13.79 MPa for 4 passes), droplet disruption would be severe within the interaction chamber. Thus, new interfaces were formed and re-coalesced due to high-intensity turbulence, which finally caused droplet collision. Moreover, droplet size increased if re-coalescence exceeded disruption.[7] Therefore, a balance between droplet disruption and further re-coalescence was required for effective microfluidization of emulsion. The deteriorating effect of dynamic high-pressure homogenization involves rapid and intense pressure changes caused by several factors such as cavitation, shear force, turbulence and temperature fluctuations.[39] These forces simultaneously affect the functional properties of proteins by including conformational changes and molecular degradation, leading to poorer adsorption at the interface.

For ultrasonication, emulsion ultrasonicated at 50% amplitude for 10 min had a smaller droplet size, followed by emulsions prepared using 40% amplitude for 15 min ($p < 0.05$). However, with further increase in sonication time from 10 to 15 min at 50% amplitude, some larger droplets were formed and PDI was increased due to the overprocessing effect ($p < 0.05$). Thus, to avoid the detrimental effects of ultrasonication, an optimal energy input should be determined. These differences were more evident in d_{32} than d_{43} for most samples. In general, d_{32} is inversely proportional to the specific surface area. The smaller d_{32} contributes to a greater specific surface area, which enhances protein adsorption at the interface.[34] The result coincided with the APC of the emulsions (Fig. 2). In addition, d_{43} is used as the index of coalescence and flocculation.[8] Emulsion ultrasonicated at 50% amplitude had smaller droplet sizes than those emulsified at 40% amplitude ($p < 0.05$). Increasing amplitude enhanced cavitation, thereby generating more bubbles due to frequent liquid thread breakage.[7] Furthermore, the energy input in the system might raise the temperature, thus facilitating the dispersion of both liquid phases into one another through decreases in interfacial tension, viscosity, and Laplace pressure. This resulted in smaller droplets.[35] On the other hand, when 40% amplitude was applied, droplet size decreased with the augmenting sonication time (from 5 to 15 min) ($p < 0.05$). Prolonged sonication induced the excellent mixing between oil and aqueous phase, due to extended turbulent flow. As a result, more droplets were effectively disrupted, which could result in more stable emulsion.[20] The result was in accordance with ESI (Fig. 1B). Hence, ultrasonication has the potential to produce more stable SO-in-water nanoemulsions with smaller droplets and lower PDI than microfluidization. Smaller droplet sizes directly contribute to a more stable emulsion due to their increased surface area to volume ratio.[34] This larger interfacial area allows for more effective coverage by emulsifiers, preventing droplet coalescence. Additionally, smaller droplets are less affected by gravitational force, reducing the tendency for creaming or sedimentation, thus contributing to enhanced storage stability.[7]

3.5. ζ-potential

The ζ-potential of the microfluidized emulsions (15–20 mV) was lower than that of the ultrasonicated emulsions (22–28 mV) ($p < 0.05$). Emulsion with low ζ-potential is regarded as unstable and quickly flocculated or coagulated droplets during storage, whereas emulsions with high ζ-potential are considered more stable due to a greater rate of repulsive forces than attractive forces between droplets.[26] The electrical repulsion and attraction at the surface of suspended particles were measured using the ζ-potential. Because of the repulsion across droplet surfaces, a higher positive or negative ζ-potential value has more electrostatic repulsion, thereby avoiding coalescence.[40]

When coagulation occurs among the protein molecules, the repulsive forces are reduced as indicated by reduced ζ-potential value. This happened in the sample prepared at lower input energy.[41] Instead, the emulsion prepared at optimal conditions such as microfluidization at 13.79 MPa for 2 passes and ultrasonication at 50% amplitude for 10 min had the highest electrostatic repulsion, which was associated with high stability of emulsion. The higher ζ-potential value might also be related to their smaller droplet size and lower PDI.

3.6. Microstructure

The impact of microfluidization and ultrasonication on the microstructure of SO nanoemulsion is illustrated in Fig. 4. Larger droplet size was found in emulsion processed at low input energy for both microfluidization (6.89 MPa for 2 passes) and ultrasonication (40% amplitude for 5 min). A significant reduction in droplet size was obtained with augmenting input energy. Optimal microscopy is a device that magnifies and captures images using optical principles, and it is used to evaluate the microstructure of emulsions.[35] Overall, ultrasonicated emulsion (50% amplitude for 10 min) had smaller droplet size and greater droplet dispersion than microfluidized emulsion under all operating conditions applied. High-frequency vibration weakened the intermolecular forces between the protein films that surrounded the oil droplets. This resulted in an increase in intermolecular distance and improved dispersion.[22] Furthermore, ultrasound-induced cavitation effects facilitated the formation of smaller droplets, thereby enhancing the stability of nanoemulsion.[28] Nevertheless, upsurge in the droplet size was noticed in ultrasonicated emulsion at high energy input (50% amplitude for 15 min). This indicated that moderate ultrasonication was beneficial to produce more stable SO nanoemulsion.

3.7. Flocculation index (F_i)

Typically, flocculation occurs naturally in the emulsion, due to the attractive interactions or aggregations between droplets.[9] The diameter of the droplets in the emulsion increased, and the emulsion stability became lowered. Index of flocculation was directly related to the emulsion stability (Table 1). F_i can be determined by d_{43} of the emulsion droplets and SDS is utilized as a dispersing agent because it prevents certain droplets from aggregating in the aqueous phase and reflects the size of every single oil droplet.[42] Ultrasonication (50% amplitude for 10 min), as a homogenization technique, yielded the emulsion with lower F_i index than microfluidization (13.79 MPa for 2 passes ($p < 0.05$)). Low F_i value suggested that the adsorbed protein layer was sufficient to counteract the stronger and more extensive van der Waals attraction.[43] Creaming phenomena were also evaluated by measuring the visual creaming index (CI). However, no significant difference was observed in CI during 15 days of storage. This indicated that both microfluidization and ultrasonication improved the creaming stability of SO nanoemulsion. Regarding emulsion stability, coalescence appeared at a very low level (data not shown). Moreover, complete coalescence did not occur in any emulsions because there was still a strong steric repulsion between droplets. The result was in line with ζ-potential (Table 1).

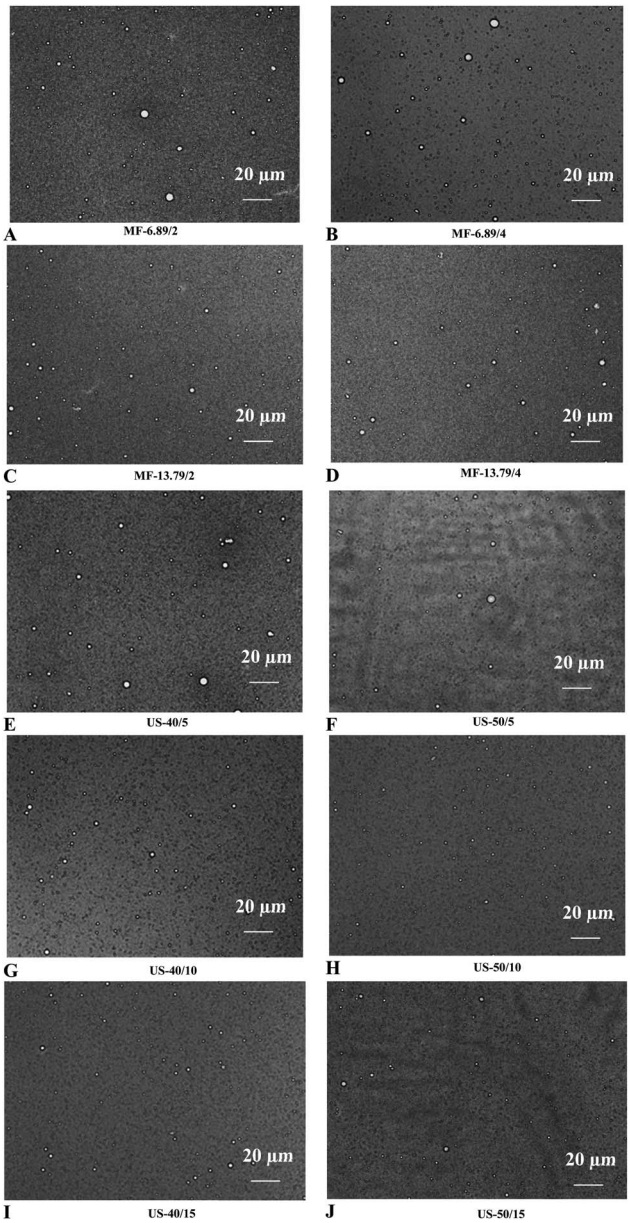

Fig. 4 Microstructure of SO nanoemulsions stabilized by fish myofibrillar protein (FMP) prepared using microfluidization (A)–(D) and ultrasonication (E)–(J) under varying operating conditions. MF-6.89/2, MF-6.89/4, MF-13.79/2, MP-13.79/4: SO nanoemulsions microfluidized at 6.89 MPa and 13.79 MPa for 2 and 4 cycles, respectively. US-40/5, US-40/10, and US-40/15, US-50/5, US-50/10, US-50/15: SO nanoemulsions ultrasonicated at 40% and 50% amplitude for 5, 10 and 15 min, respectively. Observations were made at 40× magnification.

3.8. CLSM

CLSM images of ultrasonicated (50% amplitude for 10 min) and microfluidized (13.79 MPa for 2 passes) emulsions are illustrated in Fig. 5. CLSM is commonly used to investigate the shape, aggregation, and dispersion pattern of droplets in

emulsion.[44] Regarding the dispersion pattern of droplets, ultrasonicated emulsion had a monodisperse characteristic. On the other hand, microfluidized emulsion possessed a broad range of droplet sizes termed as a polydisperse emulsion. CLSM result was in accordance with droplet size, PDI, and microstructure (Table 1 and Fig. 4). Compared with ultrasonicated emulsion, microfluidized emulsions showed obvious agglomeration, in which the larger droplets could be formed. Because of the unstable nature of the emulsion system, oil droplets and protein molecules are regularly aggregated or precipitated by the Law of Strokes.[22] As expected, oil droplets in the ultrasonicated emulsion were smaller, and uniformly dispersed with less aggregation. In addition, CLSM also validated the size of individual oil droplets, which matched the data on droplet size.

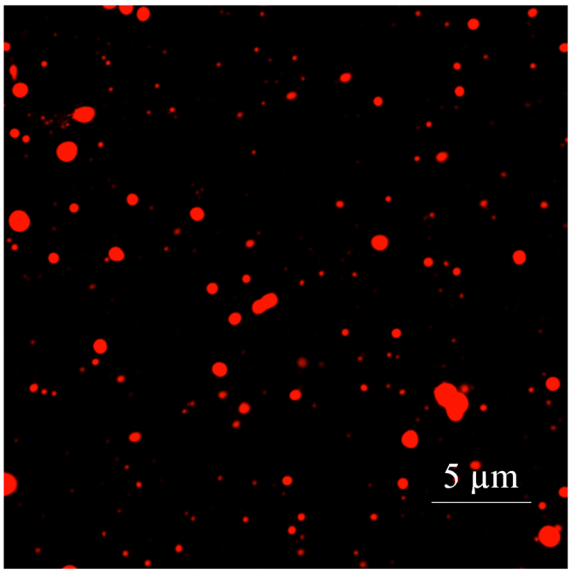

A

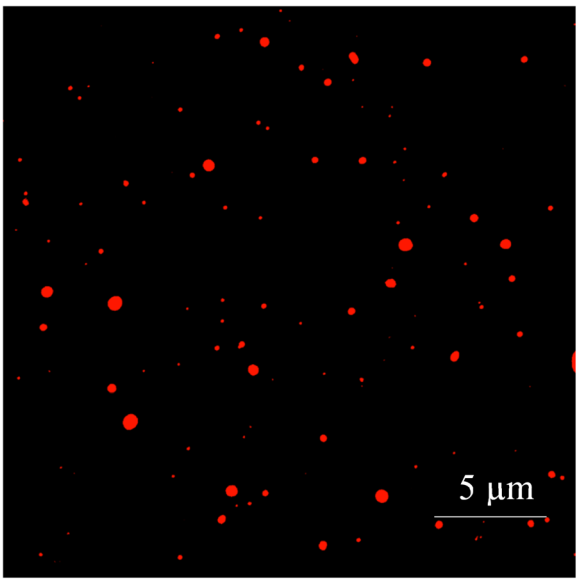

B

Fig. 5 Confocal laser scanning microscopic images of SO nanoemulsions stabilized by fish myofibrillar protein (FMP) prepared under optimal conditions of microfluidization ((A); 13.79 MPa, 2 passes) and ultrasonication ((B); 50% amplitude, 10 min). Observations were made at 400× magnification.

4. Conclusion

Both microfluidization and ultrasonication could be used to prepare stable SO nanoemulsion. Improvement in emulsifying properties, APC, thermal stability and centrifugal stability was achieved when the appropriate conditions for the operation were employed and over-processing must be avoided. Notably, the ultrasonicated emulsion demonstrated a clear advantage over the microfluidized emulsion in terms of lower droplet size, PDI, F_i and higher ζ-potential. Microstructure and CLSM images further confirmed these advantages, underlining the potential of ultrasonication as an efficient method for the production of stable SO nanoemulsion. These nanoemulsions could be utilized as functional foods *e.g.*, mayonnaise, *etc.*

Data availability

Data were not shared.

Author contributions

Bharathipriya Rajasekaran: data curation; investigation; methodology; writing original draft. Avtar Singh: conceptualization; supervision; data curation; writing-review & editing. Krisana Nilsuwan: data curation; writing-review & editing. Lukai Ma: data curation; writing-review & editing. Rasool Abdul Nazeer: conceptualization; supervision; writing-review & editing. Soottawat Benjakul: conceptualization; funding acquisition; resources; supervision; writing-review & editing.

Conflicts of interest

The authors have declared no conflicts of interest.

Acknowledgements

This research was supported by the National Science, Research and Innovation Fund (NSRIF) and Prince of Songkla University (PSU) (Grant No. AGR6505155M). PSU president scholarship for Bharathipriya Rajasekaran, Prachayacharn grant from PSU (Grant No. AGR6602079No.) and chair professor grant (Grant No. P-20-52297) are gratefully acknowledged.

References

1 O. K. Ozturk and H. Turasan, *Trends Food Sci. Technol.*, 2021, **116**, 609–625.
2 S. Takeungwongtrakul, S. Benjakul, J. Santoso, W. Trilaksani and M. Nurilmala, *J. Food Process. Preserv.*, 2015, **39**, 10–18.

3 S. Gulzar, N. Raju, R. C. Nagarajarao and S. Benjakul, *Trends Food Sci. Technol.*, 2020, **100**, 307–319.
4 H. Hosseini and S. M. Jafari, *Adv. Colloid Interface Sci.*, 2020, **282**, 102210.
5 D. Li, Z. Wei and C. Xue, *Compr. Rev. Food Sci. Food Saf.*, 2021, **20**, 5345–5369.
6 L. Zhou, J. Zhang, L. Xing and W. Zhang, *Trends Food Sci. Technol.*, 2021, **110**, 493–512.
7 N. A. McCarthy, D. Kennedy, S. A. Hogan, P. M. Kelly, K. Thapa, K. M. Murphy and M. A. Fenelon, *Food Res. Int.*, 2016, **89**, 415–421.
8 B. Rajasekaran, A. Singh, B. Zhang, H. Hong and S. Benjakul, *Eur. J. Lipid Sci. Technol.*, 2022, **124**, 2200068.
9 Y.-Y. Zhao, P. Wang, Y.-F. Zou, K. Li, Z.-L. Kang, X.-L. Xu and G.-H. Zhou, *Food Res. Int.*, 2014, **58**, 98–104.
10 M.-A. Mehrnia, S.-M. Jafari, B. S. Makhmal-Zadeh and Y. Maghsoudlou, *Int. J. Biol. Macromol.*, 2016, **84**, 261–267.
11 S. M. Jafari, Y. He and B. Bhandari, *Eur. Food Res. Technol.*, 2007, **225**, 733–741.
12 S. Gulzar and S. Benjakul, *Food Chem.*, 2020, **310**, 125916.
13 D. Zhang, Z. Wu, J. Ruan, Y. Wang, X. Li, M. Xu, J. Zhao, H. Lin, P. Liu and Z. Wang, *LWT*, 2022, **172**, 114190.
14 J. Carpenter and V. K. Saharan, *Ultrason. Sonochem.*, 2017, **35**, 422–430.
15 S. Chanarat, S. Benjakul and A. H-Kittikun, *J. Sci. Food Agric.*, 2012, **92**, 844–852.
16 H. W. Robinson and C. G. Hogden, *J. Biol. Chem.*, 1940, **135**, 707–725.
17 L. Zhou, W. Zhang, J. Wang, R. Zhang and J. Zhang, *Ultrason. Sonochem.*, 2022, **82**, 105885.
18 K. Nilsuwan, S. Benjakul and T. Prodpran, *Int. J. Food Eng.*, 2016, **12**, 647–660.
19 A. Taha, T. Hu, Z. Zhang, A. M. Bakry, I. Khalifa, S. Pan and H. Hu, *Ultrason. Sonochem.*, 2018, **49**, 283–293.
20 L. H. Sun, S. W. Lv, C. H. Chen and C. Wang, *Cereal Chem.*, 2019, **96**, 478–486.
21 M. Silva, B. Zisu and J. Chandrapala, *Food Chem.*, 2020, **309**, 125758.
22 T. Wang, N. Wang, N. Li, X. Ji, H. Zhang, D. Yu and L. Wang, *Ultrason. Sonochem.*, 2022, **82**, 105871.
23 T. Sae-leaw, S. Benjakul, N. M. O'Brien and H. Kishimura, *Int. J. Food Sci. Technol.*, 2016, **51**, 1204–1211.
24 S. Benjakul, U. Patil, T. Prodpran, T. Senphan and N. Cheetangdee, *Ital. J. Food Sci.*, 2017, **29**, 145–157.
25 U. Patil and S. Benjakul, *Food hydrocolloids*, 2017, **69**, 220–228.
26 K. Han, X. Feng, Y. Yang, X. Tang and C. Gao, *Innovative Food Sci. Emerging Technol.*, 2023, **83**, 103236.
27 K. Li, L. Fu, Y.-Y. Zhao, S.-W. Xue, P. Wang, X.-L. Xu and Y.-H. Bai, *Food Hydrocolloids*, 2020, **98**, 105275.
28 Y. Hu, S. Yang, Y. Zhang, L. Shi, Z. Ren, G. Hao and W. Weng, *Food Hydrocolloids*, 2022, **130**, 107684.
29 S. Gulzar, A. K. Balange, R. C. Nagarajarao, Q. Zhao and S. Benjakul, *Foods*, 2022, **11**, 1431.
30 M. Djenouhat, O. Hamdaoui, M. Chiha and M. H. Samar, *Sep. Purif. Technol.*, 2008, **62**, 636–641.
31 C.-H. Tang and F. Liu, *Food Hydrocolloids*, 2013, **30**, 61–72.
32 J. Perrier-Cornet, P. Marie and P. Gervais, *J. Food Eng.*, 2005, **66**, 211–217.
33 W. Peng, X. Kong, Y. Chen, C. Zhang, Y. Yang and Y. Hua, *Food Hydrocolloids*, 2016, **52**, 301–310.
34 O. Kaltsa, I. Gatsi, S. Yanniotis and I. Mandala, *Food Bioprocess Technol.*, 2014, **7**, 2038–2049.
35 J. Surh, E. A. Decker and D. J. McClements, *Food Hydrocolloids*, 2006, **20**, 596–606.
36 A. R. Taherian, M. Britten, H. Sabik and P. Fustier, *Food Hydrocolloids*, 2011, **25**, 868–878.
37 M. Joshi, B. Adhikari, P. Aldred, J. Panozzo, S. Kasapis and C. Barrow, *Food Chem.*, 2012, **134**, 1343–1353.
38 W. Ma, C.-H. Tang, S.-W. Yin, X.-Q. Yang, J.-R. Qi and N. Xia, *J. Food Eng.*, 2012, **113**, 136–142.
39 L. Román, M. M. Martínez and M. Gómez, *Food Res. Int.*, 2015, **74**, 72–79.
40 D. J. McClements, *Food Emulsions: Principles, Practices, and Techniques*, CRC press, 2004.
41 H. Liu, J. Zhang, H. Wang, Q. Chen and B. Kong, *Ultrason. Sonochem.*, 2021, **74**, 105554.
42 G. Xu, C. Wang and P. Yao, *Food Hydrocolloids*, 2017, **71**, 108–117.
43 X. Feng, Y. Sun, Y. Yang, X. Zhou, K. Cen, C. Yu, T. Xu and X. Tang, *LWT*, 2020, **122**, 109025.
44 Z. Zhu, W. Zhu, J. Yi, N. Liu, Y. Cao, J. Lu, E. A. Decker and D. J. McClements, *Food Res. Int.*, 2018, **106**, 853–861.